 doi:10.20944/preprints202012.0733.v1

*Article*

# Extending Quantum Probability from Real Axis to Complex Plane

**Ciann-Dong Yan [1] and Shiang-Yi Han[2,*]**

[1] Department of Aeronautics and Astronautics, National Cheng Kung University, Tainan, Taiwan; cdyang@mail.ncku.edu.tw
[2] Department of Applied Physics, National University of Kaohsiung, Kaohsiung, Taiwan; syhan.taiwan@gmail.com
* Correspondence: syhan.taiwan@gmail.com

**Abstract:** Probability is an open question in the ontological interpretation of quantum mechanics. It has been discussed in some trajectory interpretations such as Bohmian mechanics and stochastic mechanics. New questions arise when the domain of probability extends to the complex space, including the generation of complex trajectories, the definition of the complex probability, the relation of the complex probability to the real quantum probability, and so on. The complex treatment proposed here applies the optimal quantum guidance law to derive the stochastic differential (SD) equation governing the particle's random motions in the complex plane. The ensemble of the complex quantum random trajectories (CQRTs) solved from the complex SD equation is used to construct the probability distribution $\rho_c(t,x,y)$ of the particle's position over the complex plane $z = x + iy$. The correctness of the obtained complex probability is confirmed by the solution of the complex Fokker-Planck equation. The significant contribution of the complex probability is that it can be used to reconstruct both quantum probability and classical probability, and to clarify their relationship. Although quantum probability and classical probability are both defined on the real axis, they are obtained by projecting complex probability onto the real axis in different ways. This difference explains why the quantum probability cannot exactly converge to the classical probability when the quantum number is large.

**Keywords:** complex stochastic differential equation; complex Fokker-Planck equation; quantum trajectory; complex probability; optimal quantum guidance law.

## 1. Introduction

Probability is the most subtle setting in quantum mechanics which extracts information from the abstract complex wave function. Quantum mechanics opens a new age of technology and leads the revolution of computing with the significant invention of transistors. It provides GPS (Global Positioning System) the most precise time with the atomic clock, and has advanced in the medical treatment with the development of MRI (Magnetic Resonance Imagining). No doubt quantum mechanics totally changes our daily life even we have no idea why it works in that way and how to explain its mysterious properties. We are now in a position to develop some leading-age technology, such as quantum control, quantum computing, and quantum computer, and so on. Some of the latest inventions might transcend the quantum barrier and approach to the limit of the classical boundary. Therefore, some core technology may have a request for more fundamental knowledge of quantum mechanics.

There are many classical interpretations attempt to bring ontology into quantum mechanics. The hidden-variable theories introduce unobservable hypothetical entities and propose deterministic explanations of quantum mechanical phenomena. Bohmian mechanics is one of the most widely accepted hidden-variable theory. In Bohmian mechanics the particle is guided by a wave and its initial position is the hidden variable [1]. However, the non-locality was not included initially in this theory. Bohm and Vigier later modified the theory by imposing a stochastic process on the particle

 doi:10.20944/preprints202012.0733.v1

[2]. Nelson proposed a similar stochastic formulation of the quantum theory in which the phase-space representation of stochastic processes was used [3].

Ensemble interpretation, also called the statistical interpretation, is developed based on the work of Einstein [4]. It states that the quantum state vector cannot completely describe an individual system, but only an ensemble of similarly prepared systems. The double-slits interference is one of the typical quantum phenomenon, which demonstrates the wave-particle duality, and is reproduced by an ensemble of Bohmian trajectories [5-7]. However, the lack of the experimental observations of quantum trajectories makes the statistical interpretation of the pilot-wave remain a conceptual description.

The weak measurement provides a method to determine a set of average trajectories for an ensemble of particles under the minimum disturbance measure process [8, 9]. The weak values obtained by the weak measurement are beyond the real eigenvalues and have complex values with their imaginary parts relating to the rate of variation in the interference observation [10]. The average trajectories of individual photons in a double-slits interferometer were observed through the weak measurement, which provides a solid evidence for the quantum trajectory [11]. Mahler et al. observed in their experiment that the particle guided by the pilot-wave is nonlocal even its initial position is a locally defined hidden variable in Bohmian mechanics [12]. The quantum trajectories of other systems were observed through the weak measurements, which indicates that the quantum world is not purely probabilistic but is deterministic to a certain extent [13-14]. These experimental observations motive us to study how to connect the deterministic ensemble to the probability distribution on the basis of the statistical language.

In the same period, complex Bohmian mechanics, quantum Hamilton mechanics, hyper-complex quantum mechanics, stochastic quantum mechanics, and so on, discuss the particle dynamical behaviors in complex spacetime [15-27]. In recent years, some anomalous trajectories and complex probability expressions have been observed in some optical experiments. Experimentally-obtained probabilities indicated that the quantum state can be expressed by a negative or complex joint probability distribution [28]. Zhou et al., found out that the operational trajectories of a photon in some scenarios are not continuous [29]. The interference of two 16-dimensional quantum states was observed in experimental quantum-enhance stochastic simulation [30]. The PT symmetric quantum walk was experimentally realized on directed graphs with genuine photonic Fock states [31]. Hence, the random motion observations and complex probability proposed by the experiments might provide an ontological explanation to quantum mechanics.

On the other hand, the analysis of the complex random motions with trajectories described by complex probability becomes a noticeable question in recent year. The local limiting theorem for the probability distribution over the random trajectories of the complex-valued Ornstein-Uhlenbeck process was proved by Virchenko [32]. Some researchers discussed the probability density in the complex coordinate and attempted to obtain the complex probability density function from the complex-valued wave function [33-36]. The quantum probability synthesized by a single chaotic complex-valued trajectory was proposed in [37]. In Jaoude's study [38], he pointed out that any experiment can be executed on the complex probability set, which is the sum of the real set with its corresponding real probability, and the imaginary set with its corresponding imaginary probability.

In this article, we apply a new trajectory interpretation of the quantum probability in the complex plane. The nature has its method to navigate the particle to move along an optimal path with minimum energy consumption. In the control theory, this unique method is called the optimal guidance. The cost functions to be optimized might be the energy, time, temperature, and so on. To find out how does the motion of the quantum particle obey the optimal condition required by the nature, we apply the optimal control theory to derive the optimal guidance law for the quantum motion. We consider the particle as being guided by the optimal command. The optimal command is the optimal guidance law with the minimum cost-to-go function solved from the Hamilton-Jacobi-Bellman (HJB) equation [26]. The particle moves randomly under the optimal control command in the complex plane, whose dynamic behavior can be described by the complex stochastic differential (SD) equation. Because all physical quantities are considered in the complex plane, we name this

Preprints (www.preprints.org) | NOT PEER-REVIEWED | Posted: 29 December 2020 doi:10.20944/preprints202012.0733.v1

formulation of quantum mechanics as complex mechanics. The Schrödinger equation and the quantum motions guided by the complex-valued wave function can be derived and described in the framework of complex mechanics.

In this paper, we compare the SD equation in complex mechanics with the other two SD equations in Bohmian mechanics and stochastic mechanics. The similarities of three SD equations will be discussed. The compatible results between the statistical distributions obtained by complex quantum random trajectories (CQRT), real Bohmian trajectories, and the quantum probability $|\Psi(t,x)|^2$ are demonstrated by means of the harmonic oscillator. The Fokker-Planck (FP) equation in the complex plane is numerically solved by the finite-difference method to verify the correctness of the complex probability $\boldsymbol{\rho_c(t,x,y)}$ which is constructed from an ensemble of CQRTs.

Through complex probability $\rho_c(t,x,y)$, we can link quantum probability with classical probability and clarify the difference between them. The special probability distribution $\rho_c(t,x,0)$, which represents the statistical distribution of the intersections of an ensemble of CQRTs and the real axis, is shown can reproduce the quantum probability $|\Psi(t,x)|^2$**.** On the other hand, the marginal distribution $\rho_c(t,x)$ obtained by integrating $\rho_c(t,x,y)$ with respect to the imaginary part $\boldsymbol{y}$ can reproduce the classical probability. Both $\rho_c(t,x,0)$ and $\rho_c(t,x)$ are defined on the real x-axis but they are obtained by different ways from $\rho_c(t,x,y)$. The main difference between $\rho_c(t,x,0)$ and $\rho_c(t,x)$ is that the former has nodes with zero probability, while the latter does not. Since the probability distribution of the classical harmonic oscillator does not contain any node, we find that when the quantum number $\boldsymbol{n}$ is large, $\rho_c(t,x)$ is closer to the probability defined in classical mechanics than the quantum probability $\rho_c(t,x,0)=|\Psi_n(t,x)|^2$. That is to say, $\rho_c(t,x)$ obtained from the complex probability $\boldsymbol{\rho_c(t,x,y)}$ can demonstrate the spirit of correspondence principle better than quantum probability $\boldsymbol{|\Psi_n(t,x)|^2}$.

The paper is organized as follows. The comparisons between Bohmian mechanics, stochastic mechanics and complex mechanics will be introduced in Section 2, where the similarities and differences of osmotic velocities and FP equations are discussed. The ensembles of trajectories given by Bohmian mechanics and complex mechanics are presented and compared with the quantum probability in Section 3. Section 4 solves the FP equation in the complex plane to confirm the correctness of the statistical distribution constructed by the CQRTs. Section 5 presents conclusions and discussions with a chart to concisely summarize the main findings of this article.

## 2. Real and Complex Random Motions

### *2.1. Real Random Motion in Bohmian Mechanics*

In quantum mechanics, the time evolution of a one-dimensional quantum system is described by the Schrödinger equation

$$-i\hbar\frac{\partial\Psi(t,x)}{\partial t}=\frac{\hbar^2}{2m}\nabla^2\Psi(t,x)+U\Psi(t,x), \tag{1}$$

By expressing the wavefunction in the form of

$$\Psi(t,x)=R_B(t,x)e^{iS_B(t,x)/\hbar},\quad R_B,S_B,x\in\mathbb{R}, \tag{2}$$

Equation (1) can be separated into real and imaginary parts as

$$\frac{\partial S_B}{\partial t}+\frac{\nabla S_B}{2m}+U-\frac{\hbar^2}{2m}\frac{\nabla^2 R_B}{R_B}=0, \tag{3}$$

$$\frac{\partial R_B}{\partial t}=-\frac{1}{m}\nabla S_B\nabla R_B-\frac{R_B}{2m}\nabla^2 S_B, \tag{4}$$

which are known as the quantum Hamilton-Jacobi (QHJ) equation and the continuity equation, respectively. Bohm made an assumption that the particle's motion is guided by the law [1]:

$$p_B=mv_B=\nabla S_B. \tag{5}$$

This guidance law yields an unexpected motionless situation in eigenstates in some quantum systems. This motionless issue was resolved later by considering a random collision process [2]. The random motion of a particle in such a process can be addressed as

$$dx=v_B dt+Ddw, \tag{6}$$

Preprints (www.preprints.org) | NOT PEER-REVIEWED | Posted: 29 December 2020 doi:10.20944/preprints202012.0733.v1

where $D = \sqrt{\hbar/2m}$ is the diffusion coefficient, $dw$ is the standard Wiener process, and $v_B$ is the drift velocity

$$v_B = \frac{\nabla S_B}{m} + \frac{\hbar}{2m}\nabla(\ln R_B^2). \tag{7}$$

It can be shown that the probability density of the random displacement $x$ obeys the Born's rule:

$$\rho_B(t,x) = |\Psi(t,x)|^2 = |R_B(t,x)|^2, \tag{8}$$

and satisfies the FP equation,

$$\frac{\partial \rho_B(t,x)}{\partial t} = -\nabla \cdot \big(v_B \rho_B(t,x)\big) + \frac{\hbar}{2m}\nabla^2 \rho_B(t,x). \tag{9}$$

It is obvious that the continuity equation (4) is equivalent to the FP equation (9), if Equations (7) and (8) are applied.

The QHJ equation (3) determines the particle's momentum. The last term in Equation (3) is the quantum potential, $Q_B = -(\hbar^2/2m)\nabla^2 \ln\sqrt{\rho_B}$, which makes the QHJ equation differ from the classical HJ equation, and is responsible for almost all quantum phenomena. Equations (3) and (4) represent the energy conservation and probability conservation from the classical perspective. However, a particle considered in Bohmian mechanics moves along the real axis, which cannot explain why random motion in real axis must be guided by a wavefunction defined in complex domain.

### *2.2. Real Random Motion in Stochastic Mechanics*

In Nelson's stochastic mechanics approach to quantum mechanics, he showed that the Schrödinger equation can be derived from a stochastic point of view as long as a diffusion process is imposed on the considered quantum particle [3]. The SD equation in his formalism is expressed in the following form:

$$dx = b_+ dt + dw(t), \qquad x \in \mathbb{R}, \tag{10}$$

where $b_+(x(t),t)$ is the mean forward velocity, and $w(t)$ is a Wiener process. The $dw(t)$ are Gaussian with mean 0, independent of the $dx(s)$ for $s \le t$, and

$$E_t\big[dw_i(t)dw_j(t)\big] = 2\nu\delta_{ij}dt, \tag{11}$$

where $\nu = \hbar/2m$ is the diffusion coefficient, and $E_t$ is the expectation value at time $t$. In order to derive the Schrödinger equation (1), Nelson assigned the wavefunction in the following form:

$$\Psi(t,x) = e^{R_N + iS_N}, \quad R_N, S_N \in \mathbb{R}, \tag{12}$$

where subscript $N$ denotes the Nelson's stochastic approach to quantum mechanics (we use stochastic mechanics for short). The mean forward velocity $b_+$ is the sum of the current velocity $v_\rho$ and the osmotic velocity $u_\rho$, which are defined in terms of $R_N$ and $S_N$ as

$$b_+ = v_\rho + u_\rho = \frac{\hbar}{m}\nabla S_N + \frac{\hbar}{m}\nabla R_N. \tag{13}$$

Equation (10) then can be rewritten as follows,

$$dx = \frac{\hbar}{m}(\nabla S_N + \nabla R_N)dt + dw(t). \tag{14}$$

The FP equation associated with the above SD equation is

$$\frac{\partial \rho_N(t,x)}{\partial t} = -\nabla\big(b_+ \rho_N(t,x)\big) + \frac{\hbar}{2m}\nabla^2 \rho_N(t,x). \tag{15}$$

It can be shown that the solution to equation (15) is the Born's probability density

$$\rho_N(t,x) = |\Psi(t,x)|^2 = e^{2R_N}. \tag{16}$$

With the help of Equations (13) and (16), FP equation (15) can be expressed as

$$\frac{\partial R_N}{\partial t} = -\frac{\hbar}{m}\nabla S_N \nabla R_N + \frac{\hbar^2}{2m}\nabla^2 R_N, \tag{17}$$

which can be recognized as the continuity equation (4).

We note that the osmotic velocity $u_\rho$ is in connection with the probability density $\rho_N$, if we substitute $\rho_N$ for $R_N$, i.e., $u_\rho = (\hbar/2m)\nabla \ln \rho_N$. It implies that the osmotic velocity may play an important role in the trajectory interpretation to the quantum probability. The connection between

Preprints (www.preprints.org) | NOT PEER-REVIEWED | Posted: 29 December 2020 doi:10.20944/preprints202012.0733.v1

the FP equation and the continuity equation, i.e., the imaginary part of the Schrödinger equation is spotted again. The question is why in Bohmian mechanics and stochastic mechanics the FP equation is related to the imaginary part of the Schrödinger equation, while the random motion is defined on the real axis. Or in general, why is the Schrodinger equation describing real motion defined in the complex plane?

It seems that the two classical approaches to quantum mechanics, Bohmian mechanics and stochastic mechanics, are so similar to each other; however, they are essentially different. As pointed out earlier, Bohm mechanics is built on the basis of the pilot-wave concept with the postulated guidance law, $p_B = \nabla S_B$, and then a modified version arose later in order to solve the motionless condition happened in the eigenstates. This modified version indicates that the particle is not only guided by the pilot-wave (the wavefunction), but also experiences a diffusion process. On the contrary, Nelson assumed that the particle obeys a diffusion process first and then assigned a proper wavefunction to the particle's mean forward velocity. The Schrödinger equation then can be derived from the SD equation describing the diffusion process. These two similar classical approaches certainly have something in common. For example, FP equations (9) and (15) in Bohmian mechanics and stochastic mechanics are identical in virtue of the relationship between two wavefunction expressions,

$$S_B(t,x) = \hbar S_N(t,x), \quad \ln R_B(t,x) = R_N(t,x). \tag{18}$$

The same solutions will be found by solving two FP equations; moreover, they have the same probability density satisfying the Born's rule:

$$\rho_B(t,x) = \rho_N(t,x) = |\Psi(t,x)|^2. \tag{19}$$

The SD equations proposed by Bohm and Nelson reconstruct Born's probability density through random motions on the real axis. In the next subsection, we will define particle's random motion in the complex plane to better reflect the complex nature of the Schrödinger equation.

### *2.3. Complex Random Motion in Complex Mechanics*

Let us consider a random motion taken place in the complex plane $z = x + iy$,

$$dz = u(t,z)dt + \sqrt{\nu}dw, \tag{20}$$

where $\nu$ represents the diffusion coefficient, $u(t,z)$ is the drift velocity to be determined and $w$ is the normalized Wiener process satisfying $E(w) = 0$ and $E(dw^2) = dt$. There are two displacements in Equation (20): $u(t,z)dt$ is the drift displacement, and $\sqrt{\nu}dw$ represents the random diffusion displacement. To find the optimal drift velocity $u(t,z)$, we minimize the cost-to-go function:

$$V(t,z) = \min_{u[t,t_f]} J(t,z,u) = E_{t,z}\left\{\int_t^{t_f} L\big(\tau.z(\tau),u(\tau)\big)\,d\tau\right\}, \tag{21}$$

where $E_{t,z}\{\cdot\}$ denotes the expectation over all random trajectories starting from $z(t) = z$. The expectation is needed for dealing with the randomness of the cost-to-go function. It can be shown that the optimal cost-to-go function $V(t,z)$ satisfies the stochastic HJB equation [26]:

$$-\frac{\partial V(t,z)}{\partial t} = \min_u\left\{L(t,z,u) + \nabla V(t,z)u + \frac{\nu}{2}\nabla^2 V(t,z)\right\}. \tag{22}$$

Under the demand of minimizing the terms inside the brace at the fixed time $t$ and the fixed position $z$, the optimal command $u^*(t,z)$ can be determined from the condition:

$$\frac{\partial L(t,z,u)}{\partial u} = -\nabla V(t,z), \tag{23}$$

Therefore, the stochastic HJB equation is reduced to

$$-\frac{\partial V(t,z)}{\partial t} = L(t,z,u^*) + \nabla V(t,z)u^* + \frac{\nu}{2}\nabla^2 V(t,z). \tag{24}$$

One can derive the Schrödinger equation from the above stochastic HJB equation by choosing $L(t,z,u) = mu^2/2 - U(z)$ as the Lagrangian of a particle with mass $m$ moving in the potential $U(z)$,

Preprints (www.preprints.org) | NOT PEER-REVIEWED | Posted: 29 December 2020 doi:10.20944/preprints202012.0733.v1

and $v = -i\hbar/m$ as the diffusion coefficient. For the given Lagrangian $L(t,z,u)$, the optimal drift velocity $u^*$ can be determined from Eq. (23) as

$$u^* = -\frac{1}{m}\nabla V(t,z). \tag{25}$$

The optimal cost-to-go function $V(t,z)$ is then determined from Eq.(24) with the above $u^*$:

$$\frac{\partial V}{\partial t} - \frac{1}{2m}(\nabla V)^2 - U - \frac{i\hbar}{2m}\nabla^2 V(t,z) = 0. \tag{26}$$

In terms of the following transformations,

$$V(t,z) = -S(t,z) = i\hbar \ln \Psi(t,z). \tag{27}$$

we obtain two alternative forms of the HJB equation (26):

$$\frac{\partial S(t,z)}{\partial t} + \frac{1}{2m}\big(\nabla S(t,z)\big)^2 + U - \frac{i\hbar}{2m}\nabla^2 S(t,z) = 0. \tag{28}$$

$$-i\hbar\frac{\partial \Psi(t,z)}{\partial t} = \frac{\hbar^2}{2m}\nabla^2\Psi(t,z) + U\Psi(t,z), \tag{29}$$

where Equation (28) is the QHJ equation defined in the complex domain and Eq. (29) is the Schrödinger equation with complex coordinate $z$.

It is worthy to notice that the optimal command $u^*$ (25) represents the mean velocity of the random motion described by Eq. (20), and is related to the wavefunction as

$$u^*(t,z) = -\frac{1}{m}\nabla V(t,z) = \frac{1}{m}\nabla S(t,z) = -\frac{i\hbar}{m}\nabla \ln \Psi(t,z). \tag{30}$$

We have derived the Schrödinger equation from the HJB equation in the framework of complex mechanics. The relation between the optimal cost-to-go function $V(t,z)$ and the wavefunction $\Psi(t,z)$ in Equation (27) shows that the solution of the Schrödinger equation is associated to the solution of the HJB equation in the complex plane $z = x + iy$. Accordingly, the Schrödinger equation and the wave function are both defined in complex domain owing to the complex random motion described by Equations (20) and (30). The last term in Equation (28) is the complex quantum potential $Q$, which drives the diffusion process and can be regarded as the cause of the random motions.

By applying the optimal guidance law (30) to the SD equation (20), we obtain the random motions taken place in the complex $z$-plane,

$$dz = u^* dt + \sqrt{v}dw = \frac{1}{m}\nabla S(t,z) + \sqrt{-\frac{i\hbar}{m}}dw = -\frac{i\hbar}{m}\nabla\big(\ln\Psi(t,z)\big)dt + \sqrt{-\frac{i\hbar}{m}}dw. \tag{31}$$

From Equation (31) we can see that the optimal guidance law $u^*$ is the drift velocity, which determines the particle's mean motion in the complex plane. In order to compare three classical approaches, we map all physical quantities from the one-dimensional complex variable $z = x + iy$ to the two-dimensional real $x - y$ plane. Under this mapping, the complex action function $S(t,z)$ can be symbolically separated as

$$S(t,z) = S(t,x+iy) = S_R(t,x,y) + iS_I(t,x,y). \tag{32}$$

With the above separation and $z = x + iy$, we can rewrite the complex SD equation (31) in terms of two coupled real SD equations

$$dx = \frac{\nabla S_R(t,x,y)}{m}dt + \sqrt{\frac{\hbar}{2m}}dw, \tag{33a}$$

$$dy = \frac{\nabla S_I(t,x,y)}{m}dt - \sqrt{\frac{\hbar}{2m}}dw. \tag{33b}$$

However, in practical computation we cannot analytically separate the complex-valued wave function into two real wave functions as described by Equation (32), since they are coupled by the complex Schrödinger equation. For such a long time, physicists do not know why the Schrödinger equation is complex, including Schrödinger himself. A rational explanation might be that a quantum particle is actually moving in a complex domain, and a complex wavefunction is needed to describe its motion.

Preprints (www.preprints.org) | NOT PEER-REVIEWED | Posted: 29 December 2020 doi:10.20944/preprints202012.0733.v1

There are some similarities between three SD equations in Bohmian mechanics, stochastic mechanics, and complex mechanics. We list some comparisons in Table 1.

**Table 1.** The comparisons of the SD equations and some related terms in three mechanics.

| | **Bohmian mechanics** | **Stochastic mechanics** | **Complex mechanics** |
|---|---|---|---|
| Domain | real $x$ −axis | real $x$ −axis | complex $z = x + iy$ plane |
| Wavefunction | $\Psi(t,x) = R_B e^{iS_B/\hbar}$ | $\Psi(t,x) = e^{R_N + iS_N}$ | $\Psi(t,z) = e^{iS(t,z)/\hbar}$ |
| Drift velocity | $v_B = \frac{\nabla S_B}{m} + \frac{\hbar}{2m}\nabla(\ln R_B^2)$ | $b_+ = \frac{\hbar}{m}\nabla S_N + \frac{\hbar}{m}\nabla R_N$ | $u^* = \frac{\nabla S(t,z)}{m} = -\frac{i\hbar}{m}\nabla \ln \Psi(t,z).$ |
| SD equations | $dx = v_B dt + D dw, x \in \mathbb{R}$ | $dx = b_+ dt + dw, x \in \mathbb{R}$ | $dz = u^* dt + \sqrt{\nu} dw, z \in \mathbb{C}$ |
| PDF | $\rho_B(t,x) = \lvert\Psi(t,x)\rvert^2$ Satisfying Schrodinger Eq. | $\rho_N(t,x) = \lvert\Psi(t,x)\rvert^2$ Satisfying Schrodinger Eq. | $\rho_c(t,x,y) \neq \lvert\Psi(t,x+iy)\rvert^2$ Satisfying 2D Fokker-Planck Eq. |

We can find relationships between three different expressions of the wavefunction from Table 1,

$$S_R(t,x,0) = S_B(t,x) = \hbar S_N(t,x), \tag{34}$$

$$S_I(t,x,0) = -\hbar \ln R_B(t,x) = -\hbar R_N(t,x). \tag{35}$$

The setting of $y = 0$ means that the domain of the complex wavefunction is projected from the two-dimensional $z = x + iy$ plane onto the one-dimensional x-axis. It makes sense here since quantum mechanics, Bohmian mechanics and stochastic mechanics all consider physical scenario occurred on the real $x$ −axis for one-dimensional quantum systems. From Equations (34) and (35), and the drift velocities in Table 1, we can find the following relationships:

$$v_B = \frac{\nabla S_B(t,x)}{m} + \frac{\hbar}{2m}\nabla(\ln R_B^2(t,x)) = \frac{1}{m}\nabla S_R(t,x,0) - \frac{1}{m}\nabla S_I(t,x,0), \tag{36}$$

$$b_+ = v_\rho + u_\rho = \frac{\hbar}{m}\nabla S_N(t,x) + \frac{\hbar}{m}\nabla R_N(t,x) = \frac{1}{m}\nabla S_R(t,x,0) - \frac{1}{m}\nabla S_I(t,x,0). \tag{37}$$

The current velocity $v_\rho$ and the osmotic velocity $u_\rho$ defined in stochastic mechanics are equal to the real part and negative imaginary part of the complex velocity $u^*$ evaluated at the real axis. What attracts our attention is that the osmotic velocities defined in Bohmian mechanics and stochastic mechanics are related to the imaginary part of the complex velocity in complex mechanics. This means that Bohmian mechanics and stochastic mechanics cannot describe the quantum motions completely if the imaginary part of the complex velocity is not considered. In addition, the imaginary part of the complex velocity naturally arises from the optimization process (21), but the osmotic velocities in Bohmian mechanics and stochastic mechanics are deliberately assigned.

### 3. Extending Probability to Complex Plane

An ensemble of CQRTs solved from the SD equation (31) will be used in this section to construct the probability defined in the complex plane. Let us consider a quantum harmonic oscillator with random motions in the complex plane. According to Equation (31), its dynamic behavior can be expressed as (in dimensionless form):

$$dz = -i\nabla\big(\ln \Psi_n(t,z)\big)dt + \sqrt{1/2}\,(-1+i)\xi\sqrt{dt}. \tag{38}$$

$\Psi_n(t,z)$ is the complex-valued wavefunction of the $n^{\text{th}}$ state of the harmonic oscillator,

$$\Psi_n(t,z) = C_n H_n(z) e^{-z^2/2} e^{-i(n+1/2)t}, \tag{39}$$

where $H_n(z)$ is the Hermite polynomial and $C_n$ is a normalized constant. The real probability defined in quantum mechanics is given by the Born's rule:

$$\rho_B(t,x) = \lvert\Psi_n(t,x)\rvert^2 = [C_n H_n(x)]^2 e^{-x^2}. \tag{40}$$

To integrate Equation (38), we rewrite it in the following finite-difference form:

$$z_{j+1} = z_j - i\big(\ln \Psi_n(t,z)\big)\Delta t + \frac{-1+i}{\sqrt{2}}\xi\sqrt{\Delta t},\ \ j = 0,1,\cdots n, \tag{41}$$

where $\sqrt{\Delta t}$ stems from the standard deviation of the Wiener process $dw$, and $\xi$ is a real-valued random variable with standard normal distribution $N(0,1)$, i.e., $E(\xi) = 0$ and $\sigma_\xi = 1$. Equation (41) can be numerically separated into the real and imaginary parts as:

Preprints (www.preprints.org) | NOT PEER-REVIEWED | Posted: 29 December 2020 doi:10.20944/preprints202012.0733.v1

$$x_{j+1} = x_j + \mathrm{Im}\left(\nabla \ln \Psi_n(t_j, x_j, y_j)\right)\Delta t - \frac{\xi}{\sqrt{2}}\sqrt{\Delta t}, \quad j = 0,1,\cdots n, \tag{42a}$$

$$y_{j+1} = y_j - \mathrm{Re}\left(\nabla \ln \Psi_n(t_j, x_j, y_j)\right)\Delta t + \frac{\xi}{\sqrt{2}}\sqrt{\Delta t}, \quad j = 0,1,\cdots n. \tag{42b}$$

It is noted that we cannot set $y = 0$ directly at the beginning of the iteration process to obtain the quantum mechanical or the statistic mechanical results, which consider random motions on the real $x-$axis, because the real part $x_j$ and the imaginary part $y_j$ are coupled in Equations (42). Instead, we have to integrate Equations (42) simultaneously to acquire the complete random trajectories in the complex plane. The condition of $y = 0$ implies that we have to collect the intersections of CQRTs solved from Equations (42) and the $x-$axis.

To find the trajectory-based probability distribution of the harmonic oscillator based on Bohmian mechanics, we insert the wavefunction $\Psi_1(t,x) = \sqrt{1/2\sqrt{\pi}}\, 2xe^{-x^2/2}e^{-it}$ with real coordinate $x$ into the SD equation (6) to yield the following SD equation (in dimensionless form):

$$dx = \frac{1-x^2}{x}dt + dw. \tag{43}$$

We then obtain the Bohmian random trajectory by integrating Equation (43). Figure 1a illustrates the statistical distribution given by an ensemble of Bohmian random trajectories, which matches the quantum probability $|\Psi_1(t,x)|^2$ very well. We next consider the particle with random motions in the complex plane. The equation of motion is obtained by inserting the wavefunction $\Psi_1(t,z) = \sqrt{1/2\sqrt{\pi}}\, 2ze^{-z^2/2}e^{-it}$ with complex coordinate $z$ into Equation (38),

$$dz = i\frac{z^2-1}{z}dt + \sqrt{1/2}\,(-1+i)\xi\sqrt{dt}. \tag{44}$$

From Equation (44) we can see that there are two equilibrium points, $z = \pm 1$, which correspond to the two peaks of the quantum probability $|\Psi_1(x)|^2$, denoted by the red-solid line in Figure 1b. To compare the results of quantum mechanics and Bohmian mechanics, which consider random motion on real $x-$axis, we have to collect the intersections of the CQRTs solved from Eq. (44) and the $x-$axis, which is denoted by

$$\text{point set A} = \{x_j | (x_j, 0) \in \text{CQRTs}\} \tag{45}$$

The correlation coefficient between the statistical distribution of the point set A and the quantum distribution $|\Psi_1(x)|^2$ is up to 0.9950 as shown in Figure 1b. Hence, the statistical distribution of the ensemble of the CQRTs is consistent with results of Bohmian mechanics and quantum mechanics, when the intersections of the CQRTs and the real $x-$axis are counted.

Let us see what benefit we can have by extending the statistical range from the real axis to the complex plane. As is well-known, there are nodes with $\Psi(x) = 0$ in the quantum harmonic oscillator. In our previous work [39], we solved this so-called nodal issue in the framework of complex mechanics. The statistical method we used is to collect all the points of the CQRTs with the same real part $x$:

$$\text{point set B} = \{(x_j, y_k) | \forall (x_j, y_k) \in \text{CQRTs, for fixed } x_j\} \tag{46}$$

It can be seen that the point set A is a subset of the point set B with $y_k = 0$. The statistical distribution of $x_j$ in the point set B is demonstrated together with $|\Psi_1(x)|^2$ (i.e., point set A) in Figure 2. Apparently, the two distributions are distinct near the nodes $x_{\text{node}}$. In terms of the trajectory interpretation, the nodes are formed with zero probability, indicating that the point set A is empty when it is evaluated at $x_j = x_{\text{node}}$ as shown by the red curve in Figure 2. However, the point set B is not empty when evaluated at $x_j = x_{\text{node}}$ due to the inclusion of the extra points $(x_{\text{node}}, y_k)$ with non-zero imaginary part $y_k$. The two different ways in collecting the data points cause the discrepancy between the distributions of the two point sets near the nodes. The significant contribution made by including extra complex points in the point set B is that the statistical distribution of $x_j$ in the point set B converges to the classical probability distribution as the quantum number $n$ is large, as shown in Figure 3, where the point set B is constructed by the CQRTs solved from Equation (42) with $n = 60$. On the contrary, if the point set A is constructed from the same ensemble of CQRTs, its statistical distribution, i.e., the distribution of $|\Psi_{60}(x)|^2$, shows the existence of 60 nodes located along the real axis, which is remarkably different from the classical distribution,

Preprints (www.preprints.org) | NOT PEER-REVIEWED | Posted: 29 December 2020 doi:10.20944/preprints202012.0733.v1

as shown by the green curve in Figure 3. Therefore, the extension of the quantum probability to the complex plane is crucial to the applicability of the correspondence principle.

## 4. Solving Real and Complex Probability from Fokker-Planck Equation

In this section we will confirm the correctness of the statistical distributions of the point set A and the point set B by comparing it with the solution of the FP equation. We will solve the FP equations in Bohmian mechanics and complex mechanics for the harmonic oscillator in the $n = 1$ state. The general form of the n-dimensional SD equation reads

$$\begin{bmatrix} dx_1 \\ dx_2 \\ \vdots \\ dx_n \end{bmatrix} = \begin{bmatrix} v_1(t,x_1) \\ v_2(t,x_2) \\ \vdots \\ v_n(t,x_n) \end{bmatrix} dt + \begin{bmatrix} \sigma_{11} & \sigma_{12} & \cdots \sigma_{1m} \\ \sigma_{21} & \sigma_{22} & \cdots \sigma_{2m} \\ \vdots & \vdots & \cdots \vdots \\ \sigma_{n1} & \sigma_{n2} & \cdots \sigma_{nm} \end{bmatrix} \begin{bmatrix} dw_1 \\ dw_2 \\ \vdots \\ dw_m \end{bmatrix}, \tag{47}$$

where $\mathrm{x} = [x_1\ x_2 \cdots x_n]^T$ denotes the random displacement in the n-dimensional space, $v_i$ is the diffusion velocity $(i = 1,2,\cdots,n)$, and $dw_i$ is the Wiener process $(i = 1,2,\cdots,m)$. The joint probability density $\rho(t,x) = \rho(t,x_1,x_2,\cdots,x_n)$ describing the spatial distribution of $x_i$ satisfies the n-dimensional FP equation

$$\frac{\partial \rho(t,x)}{\partial t} = -\sum_{i=1}^{n} \partial_{x_i}[v_i(t,x)\rho(t,x)] + \frac{1}{2}\sum_{i=1}^{n}\sum_{j=1}^{n} \partial_{x_i}\partial_{x_j}[D_{ij}(t,x)\rho(t,x)], \tag{48}$$

where

$$D_{ij}(t,x) = \sum_{k=1}^{m} \sigma_{ik}\,(t,x)\sigma_{jk}(t,x). \tag{49}$$

The finite-difference method is the most common method to solve the partial differential equation by discretizing the spatial and time domains. Firstly, we will verify the correctness of our finite-difference algorithm by solving the SD equation for the duffing oscillator and comparing it with the exact solution. The two-dimensional random motion $(X(t), Y(t))$ for the duffing oscillator is governed by the following SD equations

$$\dot{Y} + 2\alpha Y + \beta X + \gamma X^3 = \sigma W(t), \qquad Y = \dot{X}, \tag{50}$$

where $W(t)$ is the random Brownian increment, and α, β, γ and σ are given constants. An exact solution of the joint probability $\rho(X,Y)$ can be found as

$$\rho(X,Y) = C\exp\left\{-\frac{2\alpha}{\sigma^2}\left(Y^2 + \beta X^2 + \frac{\gamma}{2}X^4\right)\right\}, \tag{51}$$

where $C$ is a normalized constant. The corresponding FP equation of Equation (50) is

$$\frac{\partial \rho}{\partial t} = \frac{\partial(2\alpha Y + \beta X + \gamma X^3)\rho}{\partial Y} - \mathrm{Y}\frac{\partial \rho}{\partial X} + \frac{\sigma^2}{2}\frac{\partial^2 \rho}{\partial Y^2}. \tag{52}$$

The initial distribution is chosen as the two-dimensional Gaussian distribution:

$$\rho\left(X^{(0)}, Y^{(0)}\right) = \frac{1}{2\pi\theta_1\theta_2}\exp\left\{-\left(\frac{X^{(0)} - \mu_1}{2\theta_1}\right)^2 - \left(\frac{Y^{(0)} - \mu_2}{2\theta_2}\right)^2\right\}. \tag{53}$$

Figure 4 displays the exact solution (51) and the finite-difference solution to Equation (52). The consistent result indicates that our finite-difference algorithm works very well.

Next we apply the finite-difference algorithm to solve the FP equation corresponding to the Bohmian SD equation (6) for the quantum harmonic oscillator with $n = 1$. The statistical distribution $\rho_B(t,x)$ of the Bohmian random trajectory satisfies the FP equation:

$$\frac{\partial \rho_B(t,x)}{\partial t} = \frac{x^2+1}{x^2}\rho_B(t,x) + \frac{x^2-1}{x^2}\nabla\rho_B(t,x) + \frac{1}{2}\nabla^2\rho_B(t,x), \tag{54}$$

whose finite-difference model reads

$$\rho_{B,j}^{m} = \rho_{B,j}^{m-1} + \Delta t\left(\frac{x_j^2+1}{x_j^2}\rho_{B,j}^{m-1} + \frac{x_j^2-1}{x_j^2}\frac{\rho_{B,j+1}^{m-1} - \rho_{B,j-1}^{m-1}}{2\Delta x} + \frac{1}{2}\frac{\rho_{B,j+1}^{m-1} - 2\rho_{B,j}^{m-1} + \rho_{B,j-1}^{m-1}}{(\Delta x)^2}\right). \tag{55}$$

Figure 5 shows that the numerical solution to Equation (55) is in good agreement with the quantum probability $|\Psi_1(x)|^2$. This result indicates that the quantum probability $|\Psi_1(x)|^2$ can be exactly synthesized by the real random motions satisfying the Bohmian SD equation (6); or equivalently, the quantum probability $|\Psi_1(x)|^2$ is the solution $\rho_B(t,x)$ to the FP equation (54).

Preprints (www.preprints.org) | NOT PEER-REVIEWED | Posted: 29 December 2020 doi:10.20944/preprints202012.0733.v1

We now extend the random motion of the harmonic oscillator with $n = 1$ to the complex plane $z = x + iy$. The related SD equations are

$$dx = \frac{-x^2y - y^3 - y}{x^2 + y^2}dt - \frac{1}{\sqrt{2}}dw, \tag{56a}$$

$$dy = \frac{x^3 + xy^2 - x}{x^2 + y^2}dt + \frac{1}{\sqrt{2}}dw. \tag{56b}$$

By comparing Equations (56) with the general form (47) and substituting the related terms into Equation (48), the FP equation for the joint probability $\rho_c(t,x,y)$ can be derived as

$$\frac{\partial\rho_c(t,x,y)}{\partial t} = \frac{-4xy}{(x^2+y^2)^2}\rho_c + \frac{x^2y + y^3 + y}{x^2+y^2}\frac{\partial\rho_c}{\partial x} + \frac{x + xy^2 - x^3}{x^2+y^2}\frac{\partial\rho_c}{\partial y} + \frac{1}{4}\left(\frac{\partial^2\rho_c}{\partial x^2} - 2\frac{\partial^2\rho_c}{\partial x\partial y} + \frac{\partial^2\rho_c}{\partial y^2}\right) \tag{57}$$

where $\rho_c(t,x,y)$ is the probability of finding the particle at $z = x + iy$ in the complex plane. The finite-difference model of Equation (57) is given by

$$\rho_{j,k}^m = \rho_{j,k}^{m-1} + \left[\frac{-4x_jy_k}{\left(x_j^2+y_k^2\right)^2}\rho_{j,k}^{m-1} + \frac{x_j^2y_k + y_k^3 + y_k}{x_j^2+y_k^2}\frac{\rho_{j+1,k}^{m-1} - \rho_{j-1,k}^{m-1}}{2\Delta x} + \frac{x_j + x_jy_k^2 - x_j^3}{x_j^2+y_k^2}\frac{\rho_{j,k+1}^{m-1} - \rho_{j,k-1}^{m-1}}{2\Delta y}\right.$$
$$\left. - \frac{\rho_{j+1,k+1}^{m-1} - \rho_{j+1,k-1}^{m-1} - \rho_{j-1,k+1}^{m-1} - \rho_{j-1,k-1}^{m-1}}{8\Delta x\Delta y} + \frac{\rho_{j+1,k}^{m-1} - 2\rho_{j,k}^{m-1} + \rho_{j-1,k}^{m-1}}{4(\Delta x)^2} + \frac{\rho_{j,k+1}^{m-1} - 2\rho_{j,k}^{m-1} + \rho_{j,k-1}^{m-1}}{4(\Delta y)^2}\right]\Delta t. \tag{58}$$

The numerical result is shown by the blue-dashed curve in Figure 6a, where we can see that the node at $x = 0$ for $|\Psi_1(x)|^2$ does not appear in the solution $\rho_c(t,x,y)$ to Equation (58). This means that the probability of finding a particle at the node is not zero. It is because that the particle moving in the complex plane can bypass the node $(x_{\text{node}}, 0)$, through other point $(x_{\text{node}}, y_k)$ with non-zero imaginary component $y_k$. Figure 6b shows that the numerical solution to the complex FP equation (57) is consistent with the statistical distribution of the point set B, which is generated by the CQRTs solved from the complex SD equations (56). Both curves in Figure 6b show a non-zero probability of finding the particle at the node $x = 0$.

A similar trend occurs in the state of $n = 3$, as shown in Figure 7. We can see that the statistical distribution of an ensemble of CQRTs (the black-dotted line in Figure 7a) is identical to the probability density $\rho_c(t,x,y)$ solved from the complex FP equation (the blue-dashed line in Figure 7b), and both curves deviate from the quantum probability $|\Psi_3(x)|^2$ near the nodes of $\Psi_3(x)$. This result once again shows that the occurrence of nodes is purely due to the fact that the movement of particles is restricted to the real axis by the treatment of quantum mechanics

So far, our attention of the quantum probability focuses on the real axis. In complex mechanics, the quantum particle moves randomly in the complex plane, and the probability distribution of its locations must be expressed in the complex $x - y$ plane, instead of the real axis. Figure 8 illustrates the probability distribution $\rho_c(t,x,y)$ over the complex $x - y$ plane solved from the complex FP equation (58). The inset in the figure shows the contour plot of $\rho_c(t,x,y)$, from which we can see that the joint probability $\rho_c(t,x,y)$ reaches the peaks around the points $(x,y) = (1,1)$ and $(-1,-1)$, and declines to the node at $(x,y) = (0,0)$. The 3D plot of $\rho_c(t,x,y)$ manifests that when $\sqrt{x^2+y^2} > 3$, $\rho_c(t,x,y)$ approaches zero, which means that the particle in the $n = 1$ state is bounded along the real axis as well as the imaginary axis and will not be too far from the origin. By contrast, quantum probability $|\Psi_1(x)|^2$ only concern the particles on the real axis, so it only provides the probability distribution along the x-axis.

Just like $\rho_B(t,x) = |\Psi(t,x)|^2$ gives the probability of finding a particle at position $x$ on the real axis, the joint probability density $\rho_c(t,x,y)$ gives the probability that the particle appears at the position $z = x + iy$ on the complex plane. The $\rho_c(t,x,y)$ illustrated in Figure 9 shows a more complicated probability distribution over the complex plane as the particle moves in the $n = 3$ state. If we sum the probability $\rho_c(t,x,y)$ for all the values of $y$ along a vertical line $x = x_0$ in the complex plane, we recover the 1D probability distribution $\rho_c(t,x_0)$ as shown in Figure 7. Mathematically, $\rho_c(t,x,y)$ and $\rho_c(t,x)$ have the following relation

$$\rho_c(t,x) = \int_{-\infty}^{+\infty}\rho_c(t,x,y)\,dy. \tag{59}$$

Preprints (www.preprints.org) | NOT PEER-REVIEWED | Posted: 29 December 2020 doi:10.20944/preprints202012.0733.v1

The evolution from Figure 7 (Figure 6) to Figure 9 (Figure 8), i.e., from $\rho_c(t,x)$ to $\rho_c(t,x,y)$, is just the process by which we extend the definition of the quantum probability from the real axis to the complex plane.

The complex probability is a puzzle in the complex-extended quantum mechanics. It is so obscure and abstract and even hard to define, since the probability must be a positive number. One of the most convincing solutions is to directly extend Born's definition of probability to complex coordinates. Born's probability density $\rho_B(t,x) = |\Psi(t,x)|^2$ is originally defined on the real $x$ axis. After replacing the real coordinate x with the complex coordinate $z = x + iy$, we have a joint probability density $\rho_B(t,x,y) = |\Psi(t,z)|^2 = |\Psi(t,x+iy)|^2$. Since $|\Psi(t,x)|^2 dx$ correctly predicts the probability of finding a quantum particle in the interval between $x$ and $x+dx$ at time $t$, we naturally expect that $|\Psi(t,x+iy)|^2 dxdy$ can provide the probability of finding a quantum particle inside the infinitesimal region spanned by $dx$ and $dy$ in the complex plane $z = x + iy$. However, such an expectation ultimately falls, because the square-integrable condition imposed on $\Psi(t,x)$ can only guarantee that $|\Psi(t,x)|^2$ is a qualified probability density, but it cannot guarantee that $|\Psi(t,x+iy)|^2$ is also qualified. To show that $|\Psi(t,z)|^2$ is not a qualified probability measure in the complex domain, the magnitude plot of $|\Psi_1(t,z)|^2$ over the complex plane $z = x + iy$ is shown in Figure 10, where we observe $|\Psi_1(t,z)|^2 \to 0$, as $|x| \to \infty$, and $|\Psi_1(t,z)|^2 \to \infty$, as $|y| \to \infty$. The observed features of $|\Psi_1(t,z)|^2$ indicate that $|\Psi_1(t,x+iy)|^2$ cannot be used as a probability measure along the imaginary axis $y$. The correct probability density $\rho_c(t,x,y)$ describing the particle's motion with $n = 1$ in the complex plane is shown in Figure 8, which is solved from the complex FP equation (57) and is significantly different from $\rho_B(t,x,y) = |\Psi_1(t,x+iy)|^2$.

In this paper, we follow de Broglie's original intention and regard the wavefunction $\Psi(t,z)$ as a guided wave that guides the motion of particles in the complex plane, rather than as a probability density $|\Psi(t,z)|^2$. When we extend the quantum probability from the real axis to the complex plane, the complex SD equation (31) plays a key role, because the CQRTs solved from it completely determine the probability distribution of the particles in the complex plane including the real axis. The complex SD equation (31) determined by the wave function $\Psi(t,z)$ can be used to describe the random motion of particles in the complex plane. Along the random trajectory of the particles, we record the number of times the particles appear at different positions in the complex plane, and then obtain the point sets A and the point set B. From the distribution in the point set A, we reconstruct the probability of particles appearing on the real axis, and confirm that the obtained probability is identical to the Born's probability $\rho_B(t,x) = |\Psi(t,x)|^2$. On the other hand, from the distribution in the point set B, we reconstruct the probability that the real-part position of the particle is equal to $x_j$, and prove that when the quantum number increases, the probability distribution of $x_j$ obtained from the point set B gradually approaches the classical probability distribution as shown in Figure 3.

## 5. Conclusions

The quantum world with the most mysterious phenomena is described by the weirdest theory, quantum mechanics. The probability throughout quantum mechanics is the resultant of the empirical observations which is so different to our familiar classical theory and also is counterintuitive. Trajectory interpretation of quantum probability is ontological, which uses the statistical methods to recover the probability from the particle's random motion. In this article, we introduce and compare three trajectory interpretations on the basis of Bohmian mechanics, stochastic mechanics, and complex mechanics. The first two mechanics consider that the particle is moving randomly along the real $x-$axis for one-dimensional quantum systems, while complex mechanics considers random motion in the complex plane $z = x + iy$. We find out that the osmotic velocities defined in Bohmian mechanics and stochastic mechanics are related to the imaginary part of the complex velocity in complex mechanics. This relation reflects that the random motion along the imaginary y-axis is responsible for the osmotic motion, and only by considering the particle's motion in the complex plane, can we obtain all the information of quantum probability.

Preprints (www.preprints.org) | NOT PEER-REVIEWED | Posted: 29 December 2020 doi:10.20944/preprints202012.0733.v1

Our research has revealed that extending quantum probability to the complex plane will not contradict the probability originally defined on the real axis, and it can even make us more aware of the origin of real probability. From the particle's random motion in the complex plane, we find the reason why the quantum probability is defined on the real axis. It turns out that the particle's position predicted by quantum mechanics is the intersection of the particle's complex trajectory and the real axis. By solving the stochastic differential equations, we collected all the intersection points of the particle's complex trajectory and the real axis, and calculated the probability distribution of these intersection points on the real axis, and find that the obtained probability is exactly the same as the Born's quantum probability.

The quantum probability established by the intersections of the complex random trajectories and the real axis has a significant feature, that is, there are many positions on the real axis where the probability to find the particle is zero, which is the so-called node. When the quantum number increases, the number of nodes on the real axis will increase. According to Bohr's correspondence principle, when the quantum number approaches infinity, the quantum probability should approach the classical probability, that is, the classical probability should show that there are infinite nodes on the real axis. However, the fact is that there is is no node with zero probability for a harmonic oscillator in classical mechanics. This contradictory result does not mean that Bohr's correspondence principle is wrong, but that we have not figured out the difference between the definition of the quantum probability and classical probability. If expressed in the language of mathematics, classical probability $\rho_c(t,x)$ is actually the result of integrating the complex probability $\rho_c(t,x,y)$ with respect to the imaginary part $y$ of the particle's position, as shown in Equation (59). The classical probability obtained in this way is not zero even at the node, i.e., $\rho_c(t,x_{\text{node}}) \neq 0$. Through the random trajectory of the particle in the complex plane, we count the probability distribution of the particle position in the complex plane to establish $\rho_c(t,x,y)$, and then obtain the classical probability $\rho_c(t,x)$ through the integral operation of Equation (59) (for discrete data, it is an addition operation). When the quantum number is large, we confirm that the classical probability obtained in the complex plane is the probability defined by classical mechanics.

Figure 11 summarizes the contribution of this paper, which uses complex random motion to integrate quantum probability, classical probability and complex probability. It is demonstrated that the three probability measures can all be established by the distribution of the particle's random positions in the complex plane, and the difference between them is only in the way of counting the particle's positions. As shown in Figure 11, the quantum probability $\rho_B(t,x_0)$ counts the number of times that the complex trajectories intersect the real axis at a certain point $(x_0,0)$; the classical probability $\rho_c(t,x_0)$ counts the number of times that the complex trajectories intersect a certain vertical line $(x_0,y)$; the complex probability $\rho_c(t,x_0,y_0)$ counts the number of times the complex trajectories pass a certain fixed point $(x_0,y_0)$ in the complex plane. After we establish the complex probability $\rho_c(t,x,y)$, we can integrate $\rho_c(t,x,y)$ with respect to $y$ to get the classical probability $\rho_c(t,x)$, and we can evaluate $\rho_c(t,x,y)$ at $y=0$ to get quantum probability $\rho_c(t,x,0)=|\Psi(t,x)|^2$. Only by defining probability in the complex plane can we see the difference between quantum probability $\rho_c(t,x,0)$ and classical probability $\rho_c(t,x)$. There are already some experiments supporting the assumption of quantum motion in the complex plane, and we believe that there will be more evidences to disclose the complex properties of the quantum world in the near future.

**Author Contributions:** Sections 2, 3, 5 by C.-D. Yang and Sections 1, 4 by S.-Y. Han.

**Acknowledgments:** The authors are particularly grateful to Y.-C. Chen and Y.-H. Lin for providing numerical solutions on SD equation and FP equation.

**Conflicts of Interest:** The authors declare no conflict of interest.

## References

1. Bohm, D. A Suggested Interpretation of the Quantum Theory in Terms of Hidden Variables. *Phys. Rev.* **1952**, *85*, 166-193.

2. Bohm, D.; Vigier, J.P. Model of the Causal Interpretation of Quantum Theory in Terms of a Fluid with Irregular Fluctuations. *Phys. Rev*. **1954**, *96*, 208-216.
3. Nelson, E. Derivation of the Schrödinger Equation from Newtonian Mechanics. *Phys. Rev*. **1966**, *150*, 1079-1085.
4. Einstein, A.; Podolsky, B.; Rosen, N. Can Quantum-Mechanical Description of Physical Reality Be Considered Complete? *Phys. Rev*. **1935**, 47, 777-780.
5. Philippidis, C.; Dewdney, C.; Hiley, B. J. Quantum Interference and the Quantum Potential. *IL NUOVO CIMENTO*. **1979**, *52*, 15-28.
6. Ghose, P.; Majumdar, A.; Guha, S.; Sau, J. Bohmian Trajectories for Photons. *Phys. Lett. A.* **2001**, 290, 205-213.
7. Sanz, A.S.; Borondo, F.; Miret-Artés, S. Particle Diffraction Studied Using Quantum Trajectories. *J. Phys.: Condens. Matter*. **2002**, *14*, 6109-6145.
8. Aharonov, Y.; Albert, D.Z.; Vaidman, L. How the result of a measurement of a component of a spin-1/2 particle can turn to be 100. *Phys. Rev. Lett*. **1988**, *60*, 1351-1354.
9. Aharonov, Y.; Botero, A. A Quantum Averages of Weak Values. *Phys. Rev. A*. **2005**, *72*, 052111.
10. Mori, T.; Tsutsui, I. Quantum Trajectories Based on the Weak Value. *Prog. Theor. Exp. Phys.* **2015**, 043A10.
11. Kocsis, S. et al. Observing the Average Trajectories of Single Photons in a Two-Slit Interferometer. *Science*. **2011**, *332*, 1170-1173.
12. Mahler, D. H. et al. Experimental Nonlocal and Surreal Bohmian Trajectories. *Sci. Adv.* **2016,** *2*, e1501466.
13. Murch, K.W.; Weber, S.J.; Macklin, C.; Siddiqi, I. Observing Single Quantum Trajectories of a Superconducting Quantum Bit. *Nature.* **2013**, *502*, 211-214.
14. Rossi, M.; Mason, D.; Chen, J.; Schliesser, A. Observing and Verifying the Quantum Trajectory of a Mechanical Resonator. *Phys. Rev. Lett.* **2019**, *123*, *163601*.
15. John, M.V. Modified de Broglie-Bohm approach to quantum mechanics. *Found. Phys. Lett.* **2002**, *15*, 329-343.
16. Goldfarb, Y.; Degani, I.; Tannor, D.J. Bohmian Mechanics with Complex Action: A New Trajectory-Based Formulation of Quantum Mechanics. *J. Chem. Phys.* **2006**,*125*, 231103.
17. Leacock, R.A.; Padgett, M.J. Hamitlon-Jacobi Theory and the Quantum Action Variable. *Phys. Rev. Lett.* **1983**, *50*, 3-6.
18. Yang, C.D. Quantum Hamilton Mechanics: Hamilton Equations of Quantum Motion, Origin of Quantum Operators, and Proof of Quantization Axiom. *Ann. Phys*. **2006**, *321*, 2876-2926.
19. Sanz, A.S.; Miret-Artés, S. Interplay of Causticity and Verticality within the Complex Quantum Hamilton-Jacobi Formalism. *Chem. Phys. Letts*. **2008**, *458*, 239-243.
20. Yang, C.D. On the Existence of Complex Spacetime in Relativistic Quantum Mechanics. *Chos. Soli. & Frac*. **2008**, *38*, 316-331.
21. Horwitz, L.P. Hypercomplex Quantum Mechanics. *Found. Phys*. **1996**, *26*, 851-862.
22. Kanatchikov, I.V. De Donder-Weyl Theory and a Hypercomplex Extension of Quantum Mechanics to Field Theory. *Rep. Math. Phys.* **1999**, *43*, 157-170.
23. Procopio, L.M. et al. Single-Photon Test of Hyper-Complex Quantum Theories Using a Metamaterial. *Nat. Commun.* **2017**, *8*, 15044.
24. Rosenbrock, H.H. A Stochastic Variational Treatment of Quantum Mechanics. *Procs: Math. Phys. Sci.* **1995**, *450*, 417-437.
25. Wang, M.S. Stochastic Interpretation of Quantum Mechanics in Complex Space. *Phys. Rev. Lett.* **1997**, *79*, 3319-3322.
26. Yang, C.D.; Chen, L.L. Optimal Guidance Law in Quantum Mechanics. *Ann. Phys.* **2013**, *338*, 167-185.
27. Lindgren, J.; Liukkonen, J. Quantum Mechanics can be Understood through Stochastic Optimization on Spacetimes. *Sci. Reps.* **2019**, *9*, 19984.
28. Suzuki, Y. et al. Measurements of Negative and Complex Probabilities with Photon Polarization. *New. J. Phys.* **2012**, *14*, 103022.
29. Zhou, Z.Q, et al. Experimental Observation of Anomalous Trajectories of Single Photons. *Phys. Rev. A*. **2017**, *95*, 042121.
30. Ghafari, F. et al. Interfering Trajectories in Experimental Quantum-Enhanced Stochastic Simulation. *Nat. Commun*, **2019**, *10*, 1630.
31. Wu, T. et al. Experimental Parity-Time Symmetric Quantum Walks for Centrality Ranking on Directed Graphs. *Phys. Rev. Lett.* **2020**, *125*, 240501.

32. Virchenko, Y.P.; Mazmanishvili, A.S. Probability Distribution of an Integral Quadratic Functional on the Trajectories of a Complex-Valued Ornstein-Uhlenbeck Process. *Cyber. Sys. Anal.* **2004**, 40, 899-907.
33. Barkay, H.; Moiseyev, N. Complex Density Probability in non-Hermitian Quantum Mechanics: Interpretation and a Formula for Resonant Tunneling Probability Amplitude. *Phys. Rev. A.* **2001**, *64*, 044702.
34. Chou. C.C.; Wyatt. R. E. Considerations on the Probability Density in Complex Space. *Phys. Rev. A.* **2008**, *78*, 044101.
35. John, M.V. Probability and Complex Quantum Trajectories. *Ann. Phys.* **2009**, *324*, 220-231.
36. Bender, C. M.; Hook, D. W.; Meisinger, P.N.; Wang, Q.H. Probability Density in the Complex Plane. *Ann. Phys.* **2010**, *325*, 2332-2362.
37. Yang, C. D.; Wei, C. H. Synthesizing Quantum Probability by a Single Chaotic Complex-Valued Trajectory. *Int. J. Quan. Chem.* **2016**, *116*, 428-437.
38. Jaoude, A.A. The Paradigm of Complex Probability and the Brownian Motion. *Sys. Sci. & Con. Eng.* **2015**, *3*, 478-503.
39. Yang C.D.; Han, S.Y. Trajectory Interpretation of Correspondence Principle: Solution of Nodal Issue. *Found. Phys.* **2020**. *50*, 960-976.


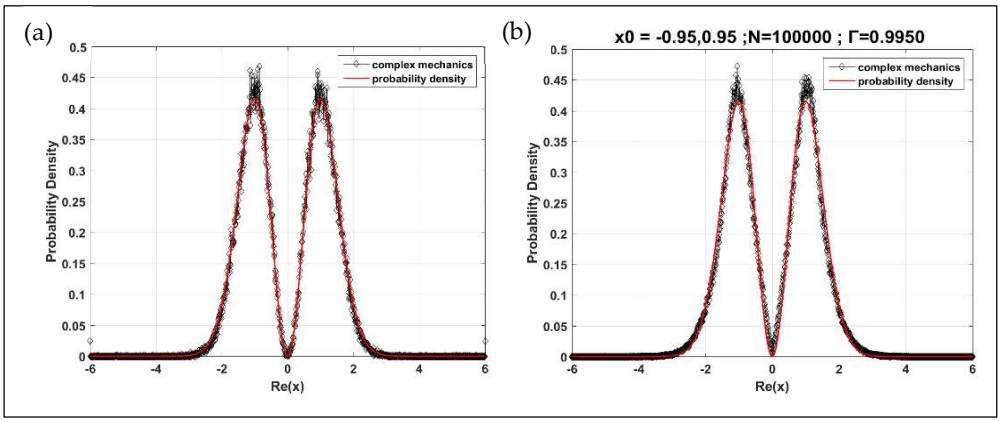


**Figure 1.** (a) The statistical distribution of an ensemble of Bohmian random trajectories for $n = 1$ state of the harmonic oscillator. The red-solid line represents the quantum probability distribution and the black-dotted line denotes the statistical distribution of the ensemble given by Bohmian mechanics. (b) The statistical distribution of an ensemble of CQRTs for $n = 1$ state is given by collecting the intersections of CQRTs and the real axis. The initial positions are $x_0 = \pm 0.95$ and there are 100,000 trajectories. The red-solid line is the quantum probability distribution and the black-dotted line is the statistical distribution of the ensemble given by complex mechanics. The correlation coefficient related to the quantum mechanical probability distribution is $\Gamma = 0.9950$.

Preprints (www.preprints.org) | NOT PEER-REVIEWED | Posted: 29 December 2020 doi:10.20944/preprints202012.0733.v1

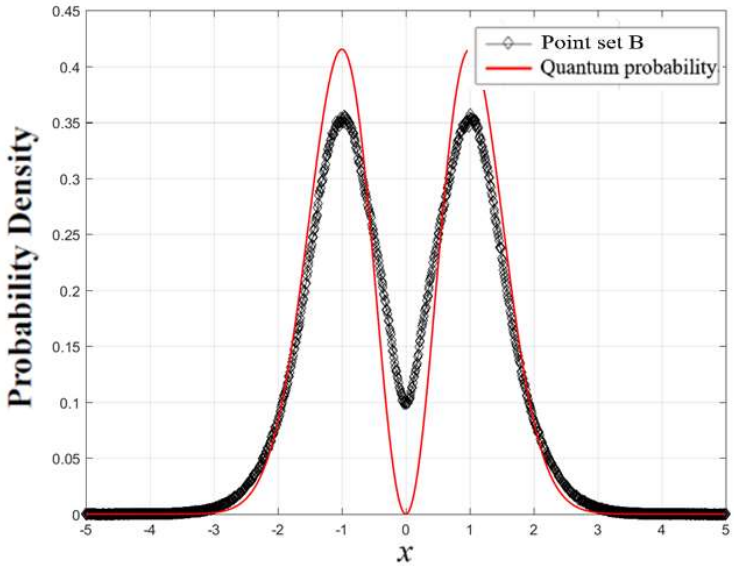


**Figure 2.** The statistical distribution of an ensemble of the intersection points and projection points on the real axis of the CQRTs for $n = 1$ state. The red-solid line is the quantum probability distribution and the black-dotted line is the statistical distribution of the point set B [39].

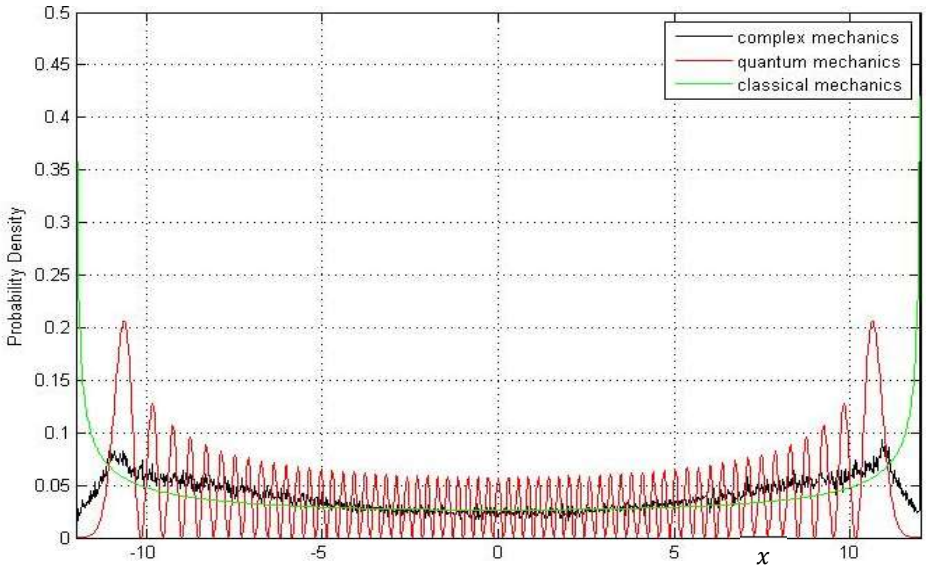


**Figure 3.** The probability distribution (black curve) constructed from an ensemble of CQRTs for the harmonic oscillator with $n = 60$ approaches the classical distribution (green curve). The quantum probability $|\Psi_{60}(t,x)|^2$ denoted by the red curve has 60 nodes located along the $x-$axis, which is remarkably different from the classical distribution.

Preprints (www.preprints.org) | NOT PEER-REVIEWED | Posted: 29 December 2020 doi:10.20944/preprints202012.0733.v1

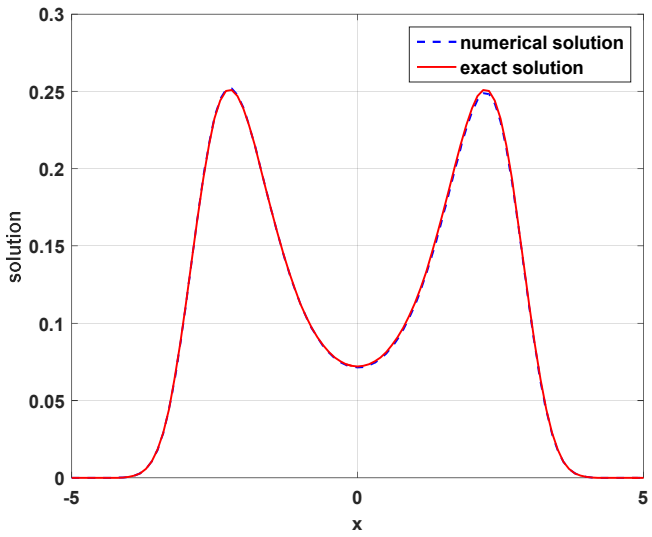


**Figure 4.** The compatible result is given by the exact solution (red-solid line) and the numerical solution (blue-dashed line) of the FP equation for one-dimensional duffing oscillator. Simulation parameters settings are: $\alpha = 0.25$, $\beta = -1$, $\gamma = 0.2$, $\sigma = 1$, $\theta_1 = \theta_2 = 0.1$, $\mu_1 = -2$, $\mu_2 = -1.8$, $dX = dY = 0.05$, and $dt = 0.0001$.

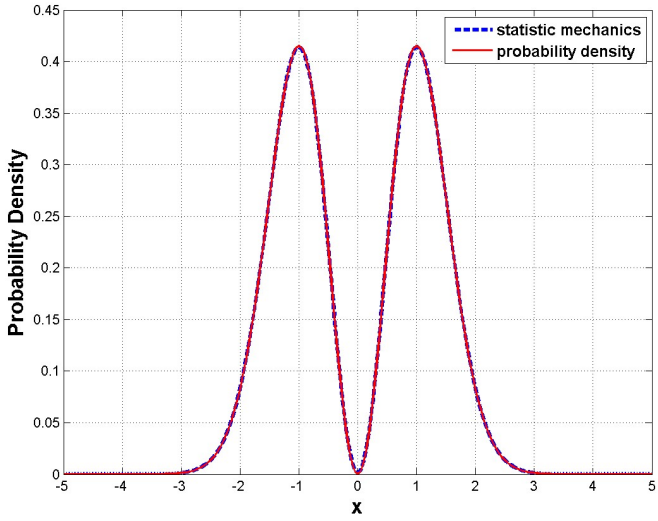


**Figure 5.** The numerical solution of the FP equation (blue-dashed line) of the harmonic oscillator in the $n = 1$ state in Bohmian mechanics is consistent with the quantum probability distribution (red-solid line). The initial probability is assigned as $\rho_B(0, x) = 2x^2 e^{-x^2}/\sqrt{\pi}$ and the boundary conditions are $\rho_B(t, -5) = \rho_B(t, 5) = 0$.

Preprints (www.preprints.org) | NOT PEER-REVIEWED | Posted: 29 December 2020 doi:10.20944/preprints202012.0733.v1

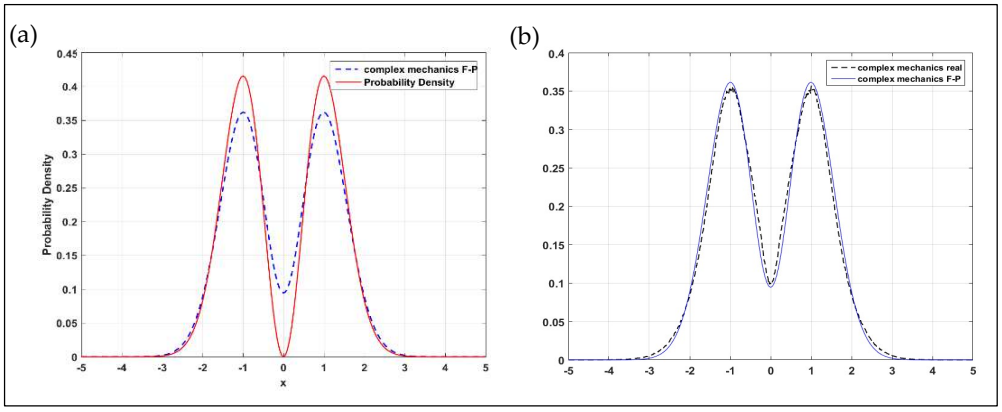


**Figure 6.** (a) The comparison of the numerical solution of the complex FP equation (blue-dashed line) to the quantum probability $|\Psi_1(t,x)|^2$ (red-solid line). (b) The comparison of the numerical solution of the complex FP equation (blue-solid line) with the statistical distribution of the point set B generated by the CQRTs for $n = 1$ state (black-dashed line). The initial probability is assigned as $\rho_c(0,x,y) = 2(x^2+y^2)e^{-(x^2+y^2)}/\sqrt{\pi}$. The boundary conditions are $\rho_c(t,-5,y) = \rho_c(t,5,y) = 0$ and $\rho_c(t,x,-5) = \rho_c(t,x,5) = 0$.

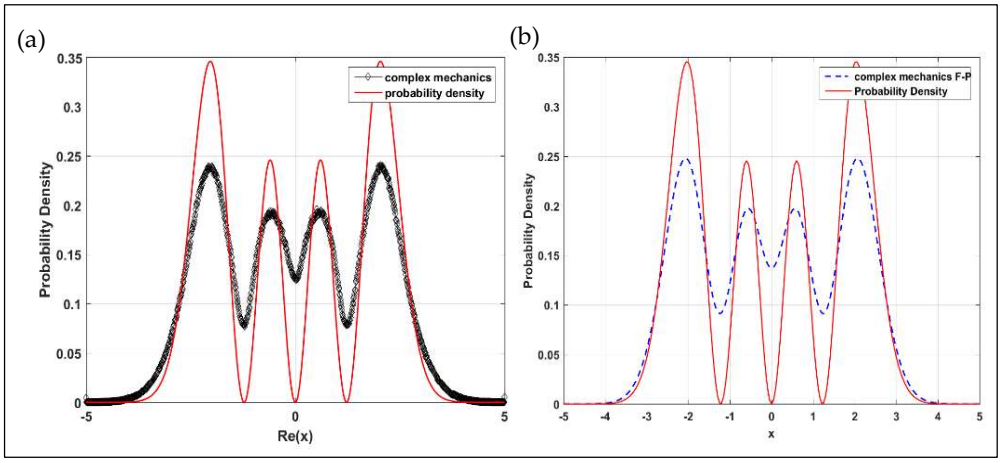


**Figure 7.** (a) The red-solid line is the quantum probability $|\Psi_3(t,x)|^2$ and the black-dotted line is the statistical distribution of the point set B generated by the CQRTs for $n = 3$ state. (b) The comparison of the solution of the complex FP equation (blue-dashed line) to the quantum probability $|\Psi_3(t,x)|^2$ (red-solid line). The initial probability is assigned as $\rho_c(0,x,y) = \left(e^{-(x^2+y^2)}/3\sqrt{\pi}\right)[4(x^6+y^6) - 12(x^4+y^4) + 9(x^2+y^2)]$. The boundary conditions are $\rho_c(t,-5,y) = \rho(t,5,y) = 0$ and $\rho_c(t,x,-5) = \rho(t,x,5) = 0$.

Preprints (www.preprints.org) | NOT PEER-REVIEWED | Posted: 29 December 2020 doi:10.20944/preprints202012.0733.v1

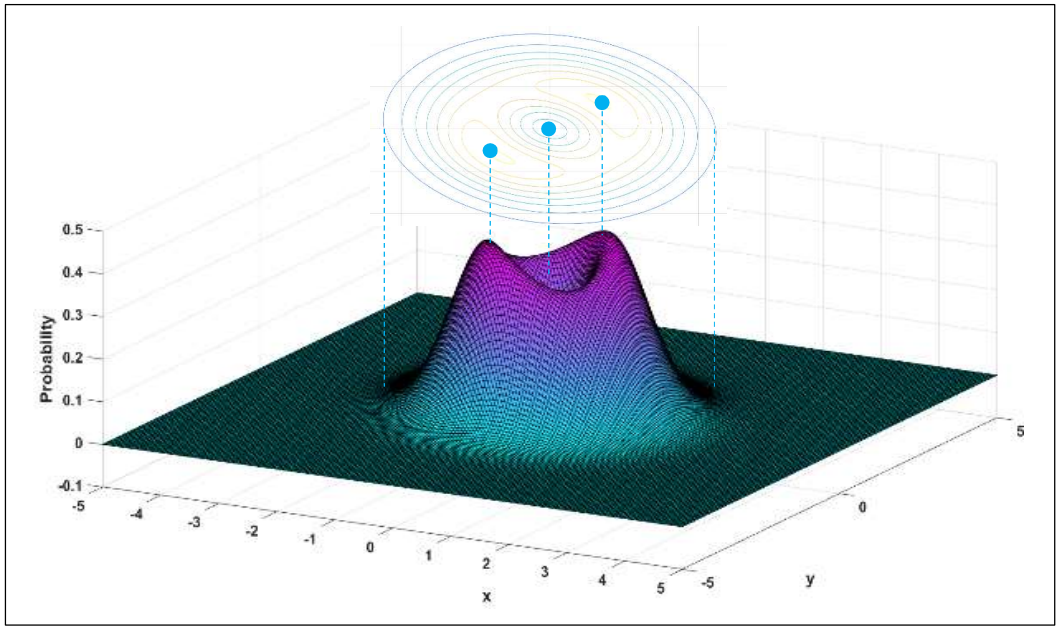


**Figure 8.** The 3D distribution and the contour of the complex probability $\rho_c(t,x,y)$ for $n=1$ state is obtained by solving complex FP equation in the $x-y$ plane.

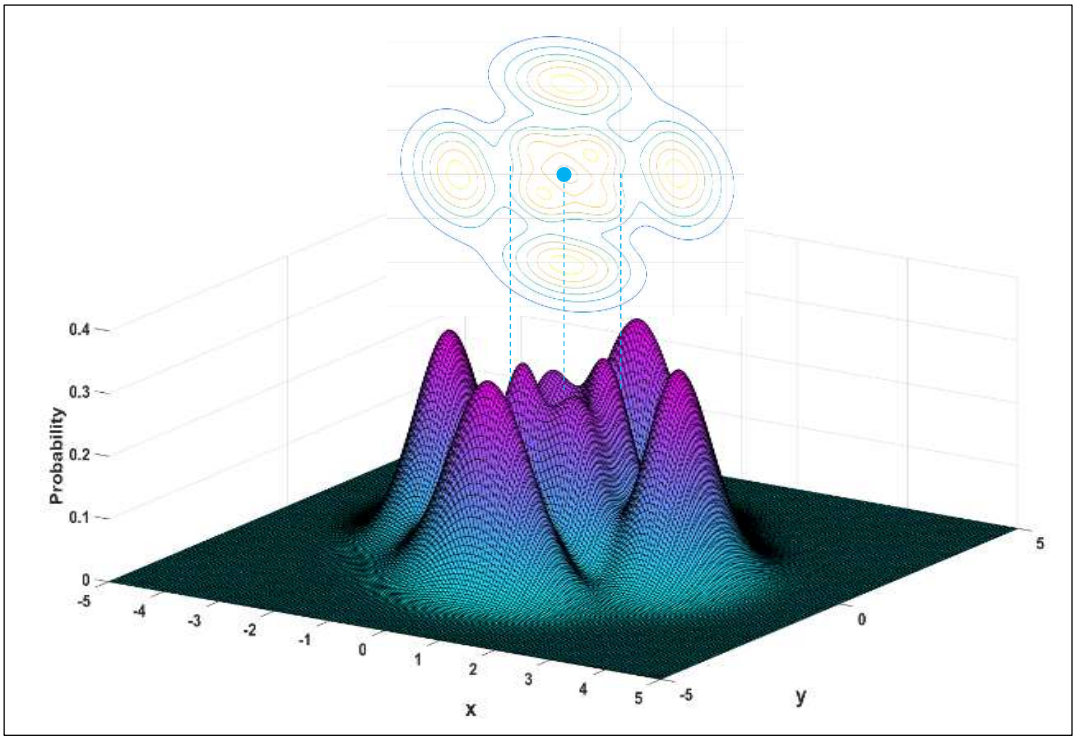


**Figure 9.** The 3D distribution and the contours of the complex probability $\rho_c(t,x,y)$ for $n=3$ state is obtained by solving the complex FP equation in the $x-y$ plane.

Preprints (www.preprints.org) | NOT PEER-REVIEWED | Posted: 29 December 2020 doi:10.20944/preprints202012.0733.v1

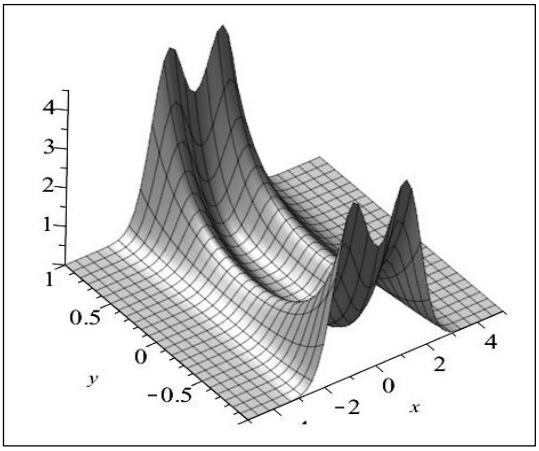


**Figure 10.** The magnitude plot of $|\Psi_1(z)|^2$ over the complex plane $z = x + iy$ shows $|\Psi_1(z)|^2 \to 0$, as $|x| \to \infty$, and $|\Psi_1(z)|^2 \to \infty$, as $|y| \to \infty$, which means that $|\Psi_1(z)|^2$ cannot be used as a probability measure along the imaginary axis.

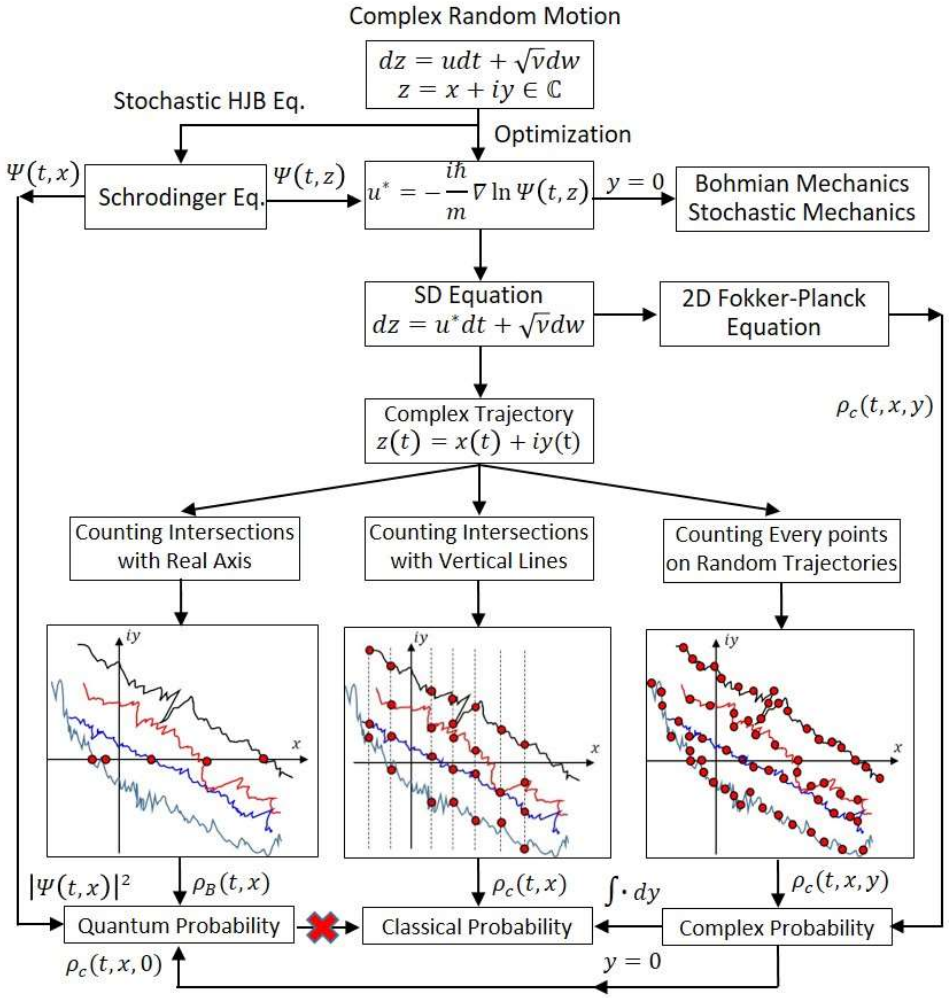


Figure 11. A chart summarizes the main findings of this article by revealing the relationships between the quantum probability, classical probability and complex probability, based on complex random motion.